ID 694

The Electron Calorimeter (ECAL) Long Duration Balloon Experiment

T. G. Guzik[1], J. H. Adams[3], G. Bashindzhagyan[4], W. R. Binns[2], J. Chang[5], M. L. Cherry[1],
M. Christl[3], P. Dowkontt[2], B. Ellison[1], J. B. Isbert[1], M. H. Israel[2], N. Korotkova[4], M. Panasyuk[4],
A. Panov[4], N. Sokolskaya[4], M. Stewart[1], J. Watts[3], J. P. Wefel[1], J. Wu[5], V. Zatsepin[4],
[1]*Louisiana State University, Baton Rouge, LA 70803, U.S.A*
[2]*Washington Universty, St. Louis, MO 63130, U.S.A.*
[3]*NASA Marshall Space Flight Center, Huntsville, AL 35812, U.S.A.*
[4]*D.V. Skobetsyn Institute of Nuclear Physics, Moscow State University ,Moscow, Russia 119992*
[5]*Purple Mountain Observatory, Nanjing, 210008, P.R. China*
guzik@phunds.phys.lsu.edu

Abstract: Accurate measurements of the cosmic ray electron energy spectrum in the energy region 50 GeV to greater than 1 TeV may reveal structure caused by the annihilation of exotic dark matter particles and/or individual cosmic ray sources. Here we describe a new long duration balloon (LDB) experiment, ECAL, optimized to directly measure cosmic ray electrons up to several TeV. ECAL includes a double layer silicon matrix, a scintillating optical fiber track imager, a neutron detector and a fully active calorimeter to identify more than 90% of the incident electrons with an energy resolution of about 1.7% while misidentifying only 1 in 200,000 protons and 0.8% of secondary gamma rays as electrons. Two ECAL flights in Antarctica are planned for a total exposure of 50 days with the first flight anticipated for December 2009.

The ECAL Science Objectives

Particle acceleration associated with supernova remnant (SNR) shocks appears to be the best (but not the only) explanation for how galactic cosmic rays (GCR) below a few PeV achieve their high energies. Evidence that particle acceleration is taking place at astrophysical sites such as SNRs is provided by electron synchrotron, gamma-ray emission measurements and cosmic ray composition measurement [1,2], but no direct detection of accelerated particles from specific sources has yet been achieved. Cosmic ray transport through the galaxy is understood to be a diffusion process, where the GCR hadronic component may traverse the distance equivalent of hundreds of galactic diameters during their lifetime, thereby randomizing their trajectory and losing connection with their original source. High energy electrons, however, have radiative energy losses that limit their lifetime and, consequently, the distance they can diffuse away from their source. As a result, the highest energy electrons that we see at Earth very likely originate from sources younger that 10^5 years and less than 1 kpc from the Solar System [3]. As there are only a handful of candidate SNRs which meet these requirements, the GCR electron energy spectrum at energies 100 GeV to ~10 TeV should show structure and allow these energetic particles to be associated with a specific (local) source.

Today, we believe that only about 5% of the universe is made up of baryonic, "ordinary", matter such as cosmic rays, while ~70% of the universe is composed of an unknown substance called "dark energy" and the remaining ~25% is made up of some form of matter that is not directly observable, i.e. "dark matter". The identity of this "dark matter" has remained a major physics mystery since Zwicky first identified the problem more than 70 years ago [4], and a myriad of investigations over the decades have essentially eliminated all known particles as dark matter candidates. Remaining choices include exotic weakly interacting species and particles that emerge from theories with extra dimensions [5]. Such particles can annihilate into electron – posi-

tron pairs and produce structure in the observed GCR electron spectrum for energies in excess of 300 GeV.

ECAL is an LDB experiment designed to investigate these two principal scientific objectives and is being developed by a collaboration between Louisiana State University (LSU), Washington University (WU) and Marshall Space Flight Center (MSFC) in the USA, Moscow State University (MSU) in Russia and Purple Mountain Observatory (PMO) in P. R. China. Here we describe the ECAL experiment details and expected performance. Another paper at this conference describes the ECAL neutron detector [6]

The ECAL Instrument

The ECAL instrument, using the ionization calorimetry technique, is designed to provide the most accurate direct measurement of cosmic ray electrons possible from an LDB platform. ECAL is an evolution of the ATIC experiment [7] augmenting the existing structure, electronics, software, detectors, and particularly the valuable, fully active Bismuth Germanate (BGO) crystal calorimeter, with new detectors to significantly enhance the separation of electrons from protons and secondary gamma rays

In an ionization calorimeter, a particle's energy is deposited inside a medium via a cascade of nuclear and electromagnetic interactions. At each step of the cascade, the energy of the primary particle is sub-divided among many secondary particles. The area under the curve of ionization energy versus depth in the medium provides a measure of the particle energy. Electron and hadron induced cascades start and develop in the instrument differently. In general, electron showers develop in direct proportion to radiation length (X_o), while hadrons must undergo a nuclear interaction to generate pions that then begin the electromagnetic cascade. Further, hadron showers usually have a wider lateral distribution of particles and a higher neutron flux relative to cascades produced by electrons. ECAL is designed to measure these different characteristics in order to maximize the distinction between electrons and protons.

A diagram of the ECAL concept payload is shown in Figure 1. The top detector in the stack that is used to determine the incident parti
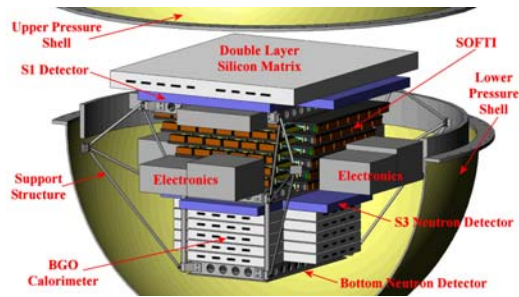

Figure 1: Diagram of the ECAL concept payload

cle charge is a highly pixilated silicon matrix of design similar to that for ATIC, but with the exception that a second layer of silicon pixels will be added. This "Double Layer Silicon Matrix" will enhance separation of electrons from secondary gamma rays, plus provide redundancy to improve the reliability of the detector. The next detector is the S1 plastic scintillator strip hodoscope that along with S3 provides the fast trigger for the instrument, as well as some redundant charge identification and particle track position information.

The Scintillating Optical Fiber Track Imager (SOFTI) is located between the S1 and S3 detectors and includes six detector planes with each plane composed of a thin sheet of lead followed by crossed X, Y layers of 1 mm scintillating optical fibers. The thickness of the lead plate in the first three layers is 1.1 mm (0.2 X_o), 1.7 mm (0.3 X_o), and 2.8 mm (0.5 X_o), while the remaining three planes will have an identical lead thickness of 5.6 mm (1.0 X_o). The planes are evenly spaced, having a top-to-bottom spacing of about 40 cm. The fiducial area of each plane has square dimensions ranging from 86 (top) to 51 cm (bottom) as shown in Figure 2. The total number of fibers in the detector is 8,222 that are formed into ribbons of 64 fibers each. Each ribbon is bonded to a cookie and coupled to a Hamamatsu R7600-M64 multi-anode photomultiplier tube
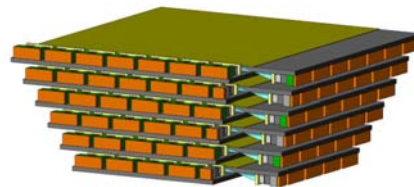

Figure 2: The SOFTI detector concept.

(MAPMT). Based on laboratory measurements using 0.75 mm fibers [8], we estimate that we should obtain ~ 9 p.e.'s respectively for minimum ionizing particles (MIP) traversing 1 mm fibers at the mean distance (40 cm) from the MAPMT and an overall detection efficiency of > 93%. SOFTI provides enhanced particle trajectory determination, further discrimination between electrons and protons, as well as between gamma rays and electrons, plus a measurement of the shower starting point.

Below SOFTI and S3 is the BGO calorimeter, which will be used, unchanged from its ATIC configuration [7]. This fully active, segmented calorimeter provides a highly accurate (~2%) measure of the incident electron energy plus measurement of the shower lateral and longitudinal distribution that is also used to distinguish between protons and electrons.

Finally, the ECAL stack includes a neutron detector that is located either just above or below the BGO calorimeter. This detector uses 2% boron loaded plastic scintillators (BC454) of total thickness 5 cm and area 50 cm by 50 cm to thermalize neutrons from the particle cascade and detect products of the $^{10}B(n,\alpha)^7Li$ reaction resulting from the capture of a thermal neutron by the ^{10}B. The time delay required to thermalize the fast neutrons allows the neutron detection to occur after the shower so that particles generated in the shower do not interfere with the neutron measurement. Simulations show that the neutron detector provides proton discrimination, independent of shower profile method, accepting 99% of all cosmic ray electron showers while rejecting about 90% of proton generated showers. Further details about the neutron detector and simulations can be found elsewhere at this conference [6].

The estimated weight of ECAL is somewhat less than 2,000 kg and includes detectors, electronics, pressure vessel, solar arrays and balloon vehicle control systems. The estimated power consumption is about 380 Watts, but taking into account power conversion efficiency about 580 Watts will be needed from the power supply. The estimated geometrical factor for ECAL varies from 0.17 m^2 sr to 0.32 m^2 sr depending upon depth in the BGO calorimeter. To obtain the statistics necessary to accomplish the stated science goals, we will need a total of about 50 flight days or two 25 day long duration balloon flights.

The Expected ECAL Performance

ECAL will be able to separate electrons from protons through differences in the shower development profile using SOFTI and the BGO calorimeter combined with the difference in neutron flux sensed by the neutron detector.

In the shower profile technique [9] an electron begins an electromagnetic shower very quickly upon entering the SOFTI target region, and deposits ~95% of its energy within the calorimeter. A proton that interacts in the instrument will have a wide spread to its secondary particles, and deposits less than ~40% of its energy in the calorimeter. Thus, at the top of the calorimeter, proton showers are wider, laterally, than electron induced showers. Near the bottom of the calorimeter electron showers are dying out while proton showers are still strong.

In SOFTI we track the particle trajectory and examine the lateral distribution in energy near the proton and electron shower core. This is illustrated in Figure 3 for a power law distribution of protons and electrons with incident energies > 1 TeV. The X-axis in the figure is the ratio, in percent, of the energy deposit in fibers within ±1 cm of the trajectory for all SOFTI layers to the total energy deposit in all the fibers of the detector. Electrons show a very tight concentration of energy around the particle trajectory while protons have a wider distribution. Placing a cut in "energy concentration" at ~60% would remove most protons while retaining most electrons.

After selection in SOFTI, the BGO calorimeter is then used to enhance the discrimination between electrons and protons. Figure 4, for a single BGO layer, shows the energy fraction, where this fraction is the ratio of the energy de
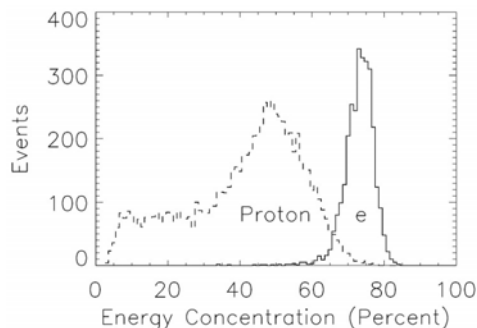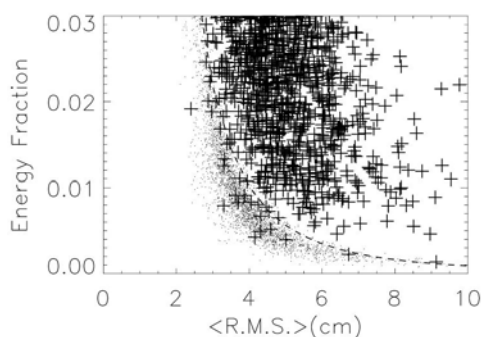

Figure 3: Energy concentration in SOFTI

Figure 4: Separation of electrons (dot) and protons (cross)

posit in the single layer to the total energy deposit in the entire calorimeter, and versus the lateral distribution R.M.S.. This figure shows that the electrons (dots) form a distinct population (below the dashed line) with a contamination of only a few of the 4×10^5 protons (plus) in the simulation. Combining such information from multiple BGO layers provides the final selection of electrons. Using this "shower profile" technique with SOFTI and the BGO calorimeter, 92% of the electrons pass the cuts while only about 20 in 4×10^5 protons remain.

The addition of the neutron detector, as mentioned earlier, provides another means to reject about 90% of the protons while retaining 99% of the electrons. Since the shower profile and neutron detection proton rejection factors are multiplicative the overall the ECAL factor is expected to be at least 1 in 200,000.
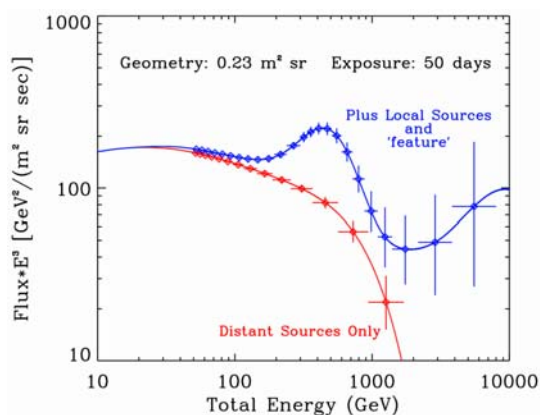

Figure 5: ECAL expected results

The expected results for ECAL are shown in Figure 5 for a geometrical factor of 0.23 m^2 sr and an exposure of 50 days. The red curve is the "distant component" curve from [3] and the blue curve is the sum of "distant" and "local components" [3] plus the preliminary feature at ~500 GeV reported by ATIC [10]. The horizontal bar on each "data" point is the energy bin width and the vertical bar is the Poisson statistical uncertainty with a confidence level of 84.13%. We expect to collect more than 25 events (corrected to the top of the atmosphere) above 1 TeV if local sources are "visible" and only about 8 events if these sources are absent. Thus, even after only one flight ECAL will be able to distinguish between the local and distant source cases at greater than 99% confidence. At lower energies statistics improve allowing energy bins to be narrowed and the features of any electron excess in the 300 GeV to 800 GeV energy range to be defined in detail. Thus, ECAL will be able to define and investigate electron spectral features up to several TeV providing high quality and significant science results over the short term to guide the observations of the space experiments.

References

[1] Higdon, J.C., *Ap. J.*, **590**, 822 (2003)

[2] Binns, W.R., *Ap. J.*, **634**, 351 (2005)

[3] Kobayashi, T., et al., *Ap. J.*, **601**, 340 (2004).

[4] Zwicky, F., *Helv. Phys. Acta*, **6**, 110 (1933).

[5] Cheng, H.C., et al., *Phys. Rev. Lett.*, **89**, 211301 (2002).

[6] Adams, J. H. et al., "A Neutron Detector for the Electron Calorimeter (ECAL) Long Duration Balloon Experiment", this conference.

[7] Guzik, T.G. et al., *Advances in Space Res.*, **33**, 1763 (2004).

[8] Rielage, K., et al., *Proc. of SPIE*, **3768**, 156-165 (1999)

[9] Adams, J. H. et al., for the ATIC Collaboration, *Proc. 26th Intl. Cosmic Ray Conf.*, Salt Lake City **5**, 41 (1999).

[10] Chang, J. et al., *Proc. 29th Intl Cosmic Ray Conf (Pune)*, **3**, 1, (2005).